Optimized Illumination Directions of Single-photon Detectors Integrated with Different Plasmonic Structures

Mária Csete*, Áron Sipos, Anikó Szalai and Gábor Szabó
Department of Optics and Quantum Electronics, University of Szeged
*Corresponding author: H-6720 Szeged, Hungary, Dom ter 9, mcsete@physx.u-szeged.hu

Abstract
The optimal orientations of different single-photon detector designs were determined by COMSOL software package. Both polar and azimuthal angles were swept during p-polarized illumination in conical-mounting. Absorption of niobium-nitride (NbN) stripes in two different (p=220 nm, 3p=660 nm) periodic patterns integrated with plasmonic elements was studied. In OC-SNSPDs consisting of ~quarter-photon-wavelength nano-cavity closed by gold reflector the optimum direction is perpendicular incidence onto NbN stripes in P-orientation. Improved absorptance is attainable in S-orientation of nano-cavity-array integrated NCAI-SNSPDs consisting of vertical and horizontal gold segments, and of nano-cavity-deflector-array integrated NCDAI-SNSPD consisting of longer vertical segments. In short-periodic NCAI-SNSPD almost polar-angle-independent perfect absorptance is achievable due to collective resonances on the MIM nano-cavity-array, while in long-periodic NCAI-SNSPD surface waves result in absorptance enhancement at specific orientations. Illumination of long-periodic NCDAI-SNSPDs at polar angle corresponding to double resonance condition makes possible to reach 82% absorptance due to **E**-field enhancement via plasmonic modes resonant in nano-cavities and propagating below NbN stripes.
Keywords: infrared photodetector, reflector, nano-cavity-array, deflector, surface waves

1. Introduction

The near-field enhancement accompanying the plasmon excitation on noble metal structures is widely applied in recent science and technology, e.g. in improvement of photo-detectors [1], and in enhancement of emission [2], as well as in laser-beam shaping [3]. The fulfillment of double resonance condition, i.e. when localized and propagating plasmonic modes are excited simultaneously on periodic arrays of resonant plasmonic objects, enables to enhance different optical phenomena, e.g. high harmonic generation [4]. Novel important application area is the improvement of supeconducting nanowire single-photon detectors (SNSPDs) detection efficiency [5]. Different noble metal elements, as simple gold reflector [6, 7], and nano-cavity-array closed by gold segments were integrated into SNSPDs [8-10]. In our previous work we have developed a numerical method based on COMSOL Multiphysics software package (COMSOL AB) and using this method we have proven that illumination of different SNSPD designs at optimum directions results in significant absorption enhancement [7, 10, 11].

The purpose of present study was the design of novel SNSPDs integrated with plasmonic structures having potential to exploit double resonance resulted phenomena via optimized geometry and illumination directions.

2. Methods

The optimum illumination directions of different SNSPD designs were determined by applying the RadioFrequency modul of COMSOL software package.

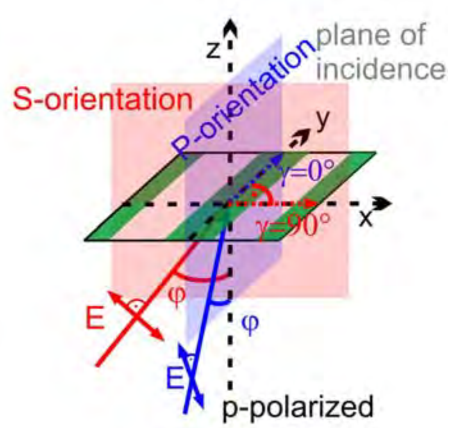

Figure 1. Schematic drawing of the illumination in case of S-orientation and P-orientation.

Absorption of niobium-nitride (NbN) stripes with parameters according to conventional SNSPDs was studied in two different periodicity regions having potential to realize absorptance maximization (p=220 nm) and parallel electrical optimization (3p=660 nm).

Port boundary condition was applied to define illumination by p-polarized light in conical mounting and Floquet periodic boundary conditions were set at the vertical sides of the models consisting of three/one unit cells of p and 3p periodic integrated patterns. Both polar and azimuthal angles were varied first, by using the parametric sweep with 5° steps in dual-angle studies, then the polar angle was tuned with 1° and 0.05° resolutions in the entire [0°-90°] region and around maxima at optimum azimuthal orientations. Finally, the time evolution of the **E**-field distribution was studied (Figure 1).

First the geometry was varied in p and 3p periodicity intervals to determine the periodicities optimal for different purposes following the principles described in Section 4.

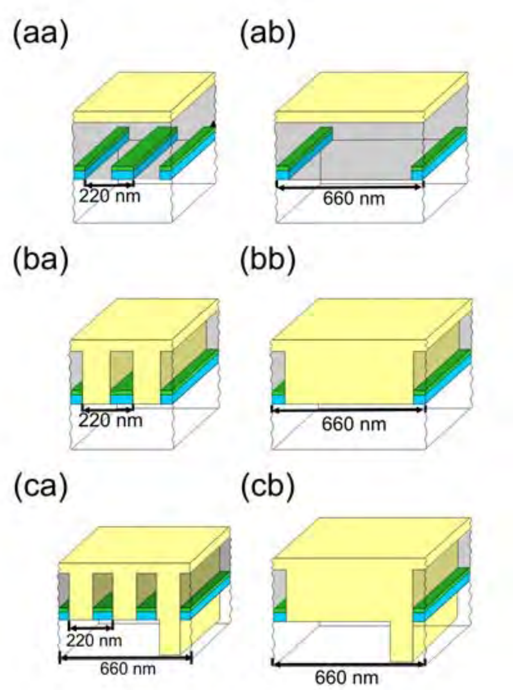

Figure 2. Schematic drawings of device designs with p = 220 nm and 660 nm periodicity in case of (aa-ab) OC-SNSPD, (ba-bb) NCAI-SNSPD, (ca-cb) NCDAI-SNSPD.

Then NbN patterns with preselected p=220 nm and 3p=660 nm periodicities were investigated in three different designs, where the absorbing NbN elements are integrated with (1) single continuous ~quarter-wavelength (279 nm long) dielectric-filled nano-optical cavity closed by a 60 nm thick gold reflector (OC-SNSPD) (Figure 2/aa-ab insets) [7], (2) array of ~quarter-plasmon-wavelength (220 nm long) nano-cavity-array closed by vertical and horizontal gold segments (NCAI-SNSPD) (Figure 2/ba-bb insets) [10], and (3) nano-cavity-deflector-array consisting of longer vertical segments (i.e. 220 nm long additional deflector) with proper 3p=660 nm periodicity (NCDAI-SNSPD) (Figure 2/ca-cb inset).

3. Theoretical Results

3.1 Dual-angle dependent optical responses

The comparative study of the optical responses and near-field distribution indicated that the optimum orientation fundamentally depends on the detector design. The optimum azimuthal orientation of both p and 3p periodic OC-SNSPDs is P-orientation (0° azimuthal angle), when the **E**-field oscillation direction is parallel to the long axes of NbN stripes (Fig. 3/aa-ab), similarly to previous OC-SNSPD studies [6, 7].

The optimum azimuthal orientation of NCAI- and NCDAI-SNSPDs is S-orientation (0° azimuthal angle), where the **E**-field oscillation direction is perpendicular to the integrated grating-like pattern made of gold (Fig. 3/ba-bb, ca-cb), similarly to the 200 nm and 600 nm designs described in [8-10].

The course of polar-angle dependent absorptance is significantly different in different designs. In OC-SNSPD slow and monotonous variation is observable when the azimuthal angle is varied in either p or 3p periodic design (Figure 3/aa-ab).

In p-periodic NCAI-SNSPD the absorptance slowly and monotonously enhances, when the azimuthal angle is increased, while in 3p-periodic NCAI-SNSPD there is a narrow polar-azimuthal angle interval, where extrema appear (Figure 3/ba-bb).

The dual-angle dependent absorptance indicates also in p-periodic NCDAI-SNSPDs noticeable modulation at these orientations, while in 3p NCDAI-SNSPD very large local absorptance enhancement appears in analogous polar-azimuthal orientations (Figure 3/ca-cb).

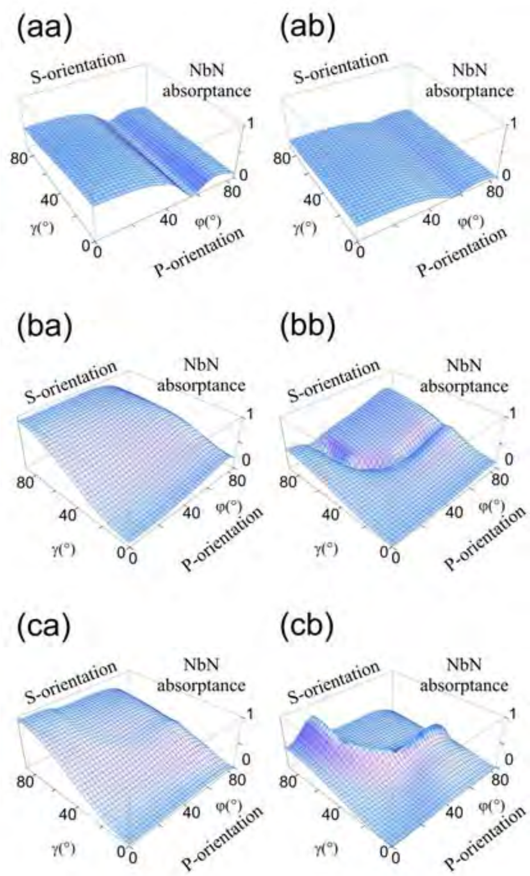

Figure 3. NbN absorptance in 220 nm and 660 nm periodic SNSPD designs (aa-ab) OC-SNSPD, (ba-bb) NCAI-SNSPD, (ca-cb) NCDAI-SNSPD.

3.2 Polar-angle dependent optical responses

The optimum illumination direction of OC-SNSPDs is perpendicular incidence onto NbN stripes in P-orientation in both p and 3p periodic designs (Fig. 4/a). The maximal absorptances are 63.8% and 28.5% indicating that the fill-factor related decrease is partially compensated due to the presence of gold reflector. There are narrow local and broad global minima on the NbN absorptance in the intervals, where surface plasmon polaritons are excited at the gold-air and gold-HSQ interfaces, i.e. the gold reflector frustrates the total internal reflection (TIR). The local NbN absorptance maxima appear at ~71°, and the corresponding reflectance signals indicate that these maxima originate from NbN-related ATIR phenomenon.

Significant absorptance improvement is attainable in S-orientation (90° azimuthal angle) of NCAI-SNSPDs (Fig. 4/b). In short periodic NCDAI-SNSPD the absorptance is 95.4 % at perpendicular incidence, which slowly and monotonously increases trough the global maximum of 95.4% reached at 44°, i.e. in the interval of ATIR. Local maximum minimum pair appears at the orientations corresponding to TIR and SPP phenomena. The corresponding optical responses indicate that the key effect of sub-wavelength periodic NCAI-SNSPD design is the reflectance suppression.

In long periodic NCAI-SNSPD the absorptance is 38.2% at perpendicular incidence. The optical response indicates dramatic changes, manifesting itself in a global minimum at 19° and a local maximum at 20.2°, where the NbN absorptance reaches 32.3 %. The global maximum (70.1%) appears at ~78° polar angle, which requires special light in-coupling method, i.e. is hardly implementable in conventional practical applications. The corresponding optical responses indicate, that the reflectance is reinforced at the orientation corresponding to the global minimum, which phenomenon is described in details in Section 4.

The wavelength-scaled periodic deflector structure integration into NCDAI-SNSPDs results in small optical response modification in short-periodic design, while dramatic and very promising nano-photonical phenomena appear in long periodic design (Fig. 4/c).

In short-periodic NCDAI-SNSPDs the NbN absorptance maximum (94.9%) is reached at perpendicular incidence, than the absorptance monotonously decreases. However in addition to the little TIR and SPR-related modulation, a steep slope appears at the orientation corresponding to the dramatic changes in long periodic design (~19.55°).

In long periodic NCDAI-SNSPD a very large absorptance maximum (82.3 %) appears at 19.55° tilting, where the reflectance is almost entirely suppressed, and the gold absorptance starts to decrease. This orientation is in between the polar angles, where the global minimum and local maximum appears on 3p periodic NCAI-SNSPDs.

The tranmittance is suppressed in all designs through the entire polar angle interval except the close proximity of the orientation corresponding to SPP excitation.

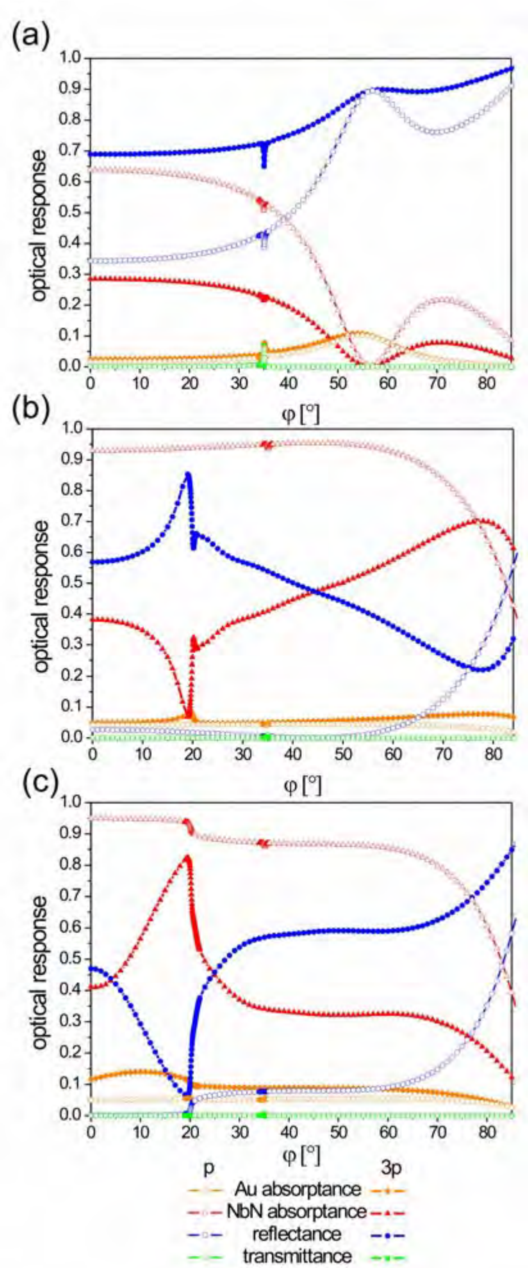

Figure 4. Optical responses in 220 nm and in 660 nm periodic SNSPD designs (a) OC-SNSPD, (b) NCAI-SNSPD, (c) NCDAI-SNSPD.

3.3 Near-field phenomena

In OC-SNSPDs the gold reflector ensures the **E**-field concentration around NbN segments aligned at the bottom of the nano-optical cavity (Fig. 5, 6/a). The **E**-field is most efficiently collected along the interface at the maximum occurring, i.e. at perpendicular incidence (Fig. 5, 6/aa), while small portion of the **E**-field is out-coupled from the nano-cavity at the 34.55° orientation corresponding to SPP excitation (Fig. 5, 6/ab).

In short periodic NCAI-SNSPD large **E**-field enhancement is observable at the bottom of each MIM nano-cavity due to excitation of resonant localized plasmonic modes (Fig. 5b) [12]. The highest **E**-field intensities are observable at the maximum of the NbN absorptance curve (Fig. /ba-to-bb). At perpendicular incidence reflected waves with weak intensity are observable on the time evolution of the **E**-field, but there are no reflected waves below the NCAI-SNSPD at the maximum.

In long-periodic NCAI-SNSPD the **E**-field intensity is strongly enhanced in the cavities (Fig. 6b), indicating that the absortance is limited by the smaller fill-factor. Interestingly, surface waves with wave fronts almost perpendicular to the interface and with ~889 nm wavelength propagate below the nano-cavity-array backward at the local maximum (Fig. 6bb). Our previous studies on 600-nm-pitch NCAI-SNSPDs have shown that these Brewster waves play important role in appearance of the local absorptance maximum [10, 11, 13].

Even tough larger local **E**-field maxima are observable in short periodic NCDAI-SNSPDs, the attainable absorptance is smaller than in NCAI-SNSPDs, caused by absorptance in deflectors (Fig. 5c). Although the **E**-field is significantly enhanced at the bottom of the nano-cavity in the closest proximity of the deflector at the tilting corresponding to inflection point on the absorptance curve, the **E**-field distribution is less advantageous compared to NCAI-SNSPDs (Fig. 5cb-to-bb). The presence of the wavelength-scaled periodic gold-deflector-array results in appearance of surface waves, which propagate back-ward at 19.55° tilting (Fig. 5cb).

In long periodic NCDAI-SNSPD similar local **E**-field enhancement is observable at perpendicular incidence at the bottom of the MIM nano-cavities, as in NCAI-SNSPDs (6ca-to-ba). Even tough the local field intensity is not further enhanced, the distribution is much more advantageous at the tilting corresponding to the large global maximum (Fig. 6cb-to-ca). The surface waves observable at this orientation below the NCDAI-SNSPD have interestingly smaller, ~ 878 nm wavelength revealing to their different plasmonic nature (Fig. 6/cb) [10, 11].

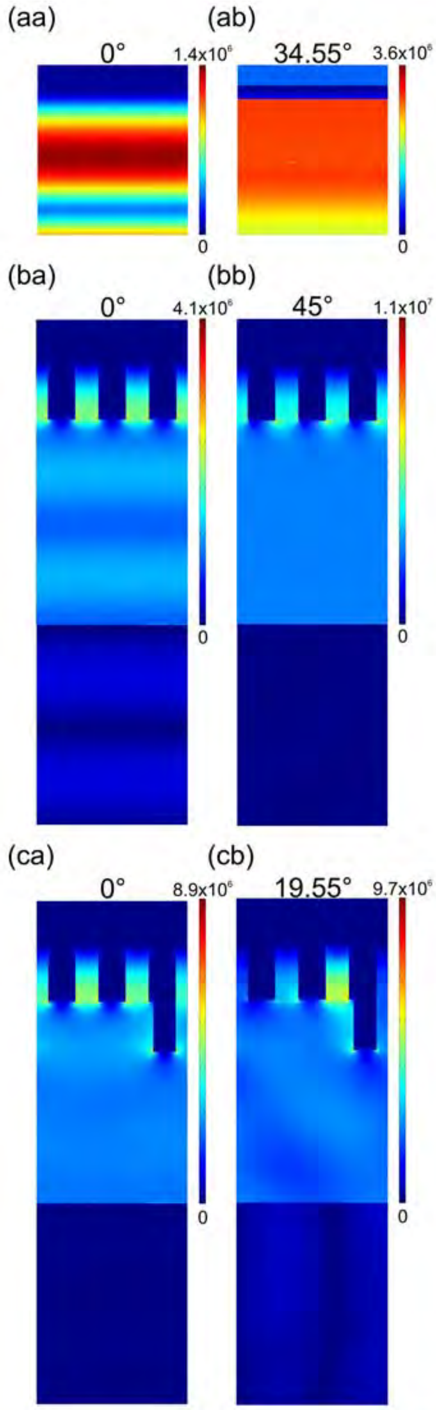

Figure 5. Near-field phenomena in 220 nm periodic design OC-SNSPD at (aa) 0° and (ab) 34.55°, NCAI-SNSPD at (ba) 0° and (bb) 45°, NCDAI-SNSPD at (ca) 0° and (cc) 19.55°. Upper parts show the normalized **E**-field, while the areas below the boundary pair indicate the $\sqrt{E_x^2 + E_y^2 + E_z^2}$ quantity.

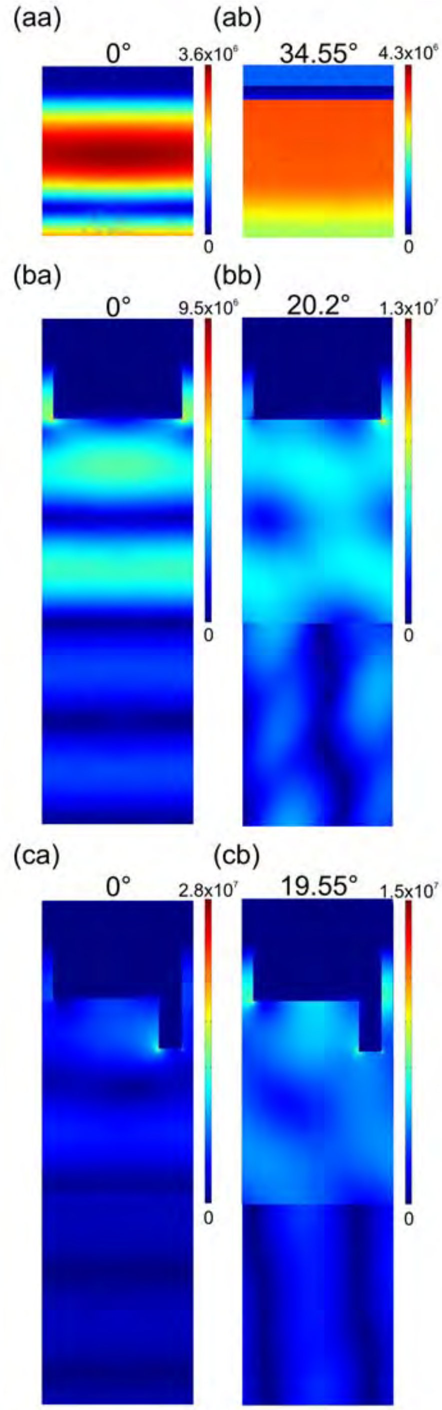

Figure 6. Near-field phenomena in 660 nm periodic design OC-SNSPD at (aa) 0° and (ab) 34.55°, NCAI-SNSPD at (ba) 0° and (bb) 20.2°, (c) NCDAI-SNSPD at (ca) 0° and (cc) 19.55°. Upper parts show the normalized E-field, , while the areas below the boundary pair indicate the $\sqrt{E_x^2 + E_y^2 + E_z^2}$ quantity.

4. Discussion

Periodicities commensurate with the wavelength of plasmons were inspected by varyingthe geometry, and the particular ~660 nm periodicity was selected, as this periodicity equals to 75% of the SPP wavelength, which is ~884 nm at NbN-sapphire and ~878 nm at gold-sapphire interface. This periodicity-plasmon-wavelength ration corresponds to the condition of resonant transmission on 1D plasmonic gratings with 3p characteristic periodicity [11, 14, 15].

Both p and 3p periodic OC-SNSPDs exhibit enhanced absorptance due to the overlapping of the **E**-field antinodes with the absorbing NbN segments at the bottom of the quarter-photonic wavelength nano-cavity. The geometry variation indicated that the 660 nm periodicity is peculiar also in these designs, according to the 75% periodicity-to-plasmon-wavelength ratio [11, 14, 15].

The NCAI-SNSPDs enable to reach larger absorptance due to the collective resonant oscillations on the MIM nano-cavity-array [10-12]. The efficiency of these collective oscillations strongly depends on the periodicity. In sub-wavelength periodicity region the collective oscillation is polar angle independent, while in wavelength-scaled designs grating-coupling phenomena results in strong perturbations at specific orientations [10, 11].

The primary computations to determine the optimal periodicity were performed, following the principle of optimal cavity illumination described in our previous studies [10, 11]. There is a coherent set of periodicities and orientations, which results synchronous illumination of different cavity series, according to Eq. (1).

$$\sin\varphi^{m,k} = \frac{m\dfrac{\lambda}{n_{sapphire}}}{k3p} \quad (1)$$

The local minimum corresponds to the m=1 and k=4 case. In 3p periodic NCDAI-SNSPDs the appropriately designed and illuminated grating enables resonant transmission. The resonantly transmitted light results in excitation of cavity resonant modes in the quarter-plasmon-wavelength nano-cavities. The global minimum appears at the orientation, where the coupling on 3p periodic grating results in backward propagating waves with wavelength (878 nm) equal to that of SPPs, while the local maximum coincides with the orientation appropriate to couple to surface waves with longer wavelength (~889 nm), e.g. to Brewster waves [11, 13].

$$\boldsymbol{k}_{surface\ wave} = \boldsymbol{k}_{photon}\sin\varphi \pm \boldsymbol{k}_{grating,3p} \quad (2)$$

At the global minimum in long periodic NCAI-SNSPD the resonant coupling to plasmons is followed by re-radiation into light, which cause the appearance of plasmonic band-gap. Orientation according to excitation to plasmons is not advantageous in 3p periodic NCAI-SNSPDs, while orientation appropriate to couple into Brewster waves is capable of resulting in local maximum.

In 3p periodic NCDAI-SNSPDs at the orientation corresponding to the global absorptance maximum the grating couples to plasmons, but the plasmons are not re-radiated into light. This is due to appropriately designed deflectors, which force the plasmonic modes to propagate backward below the NbN stripes. Finally the proper synchronization ensures the maximization of the absorptance.

5. Conclusions

The optimal geometry and illumination directions were determined for plasmonic structures integrated SNSPD designs. It was shown that the orientation of NCDAI-SNSPD at polar angle corresponding to double resonance condition is capable of compensating three times lower fill-factor related loss due to **E**-field confinement via plasmonic modes excited in cavities above and propagating below NbN stripes.

6. References

1. L. Tang, S. E. Kocabas, S. Latif, A. K. Okyay, D. S. Ly-Gagnon, K. C. Sarasvat and D. A. B. Miller, “Nanometre-scale germanium photodetector enhanced by a near-infrared dipole antenna”, *Nature Photon.*, **2**, 226-229 (2008)
2. D. E. Chang, A. S. Sorensen, P. R. Hemmer and M. D. Lukin, “Quantum Optics with Surface Plasmons”, *Phys. Rev. Lett.*, **97**, 053002 (2006)
3. N. Yu, Q. Wang, and F. Capasso: “Beam Engineering of quantum cascade lasers”, *Laser Photonics Rev*. **6** No. 1 24-26 (2012)

4. P. Genevet, J-P. Tetienne, E. Gatzogiannis, R. Blanchard, M. A. Kats, M. O. Scully, and F. Capasso, "Large enhancement of nonlinear optical phenomena by plasmonic nanocavity gratings," *Nano Letters*, **10,** 4880-4883 (2010)
5. G. N. Gol'tsman, O. Okunev, G. Chulkova, A. Lipatov, A. Semenov, K. Smirnov, B. Voronov, A. Dzardanov, C. Williams, and R. Sobolewsky, "Picosecond superconducting single-photon optical detector," *Appl. Phys. Lett.*, **79,** 705-708 (2001)
6. K. M. Rosfjord, J. K. W. Yang, E. A. Dauler, A. J. Kerman, V. Anant, B. M. Voronov, G. N. Gol'tsman, and K. K. Berggren, "Nanowire single-photon detector with an integrated optical cavity and anti-reflection coating", *Opt. Express*, **14**(2), 527-534 (2006)
7. M. Csete, Á. Sipos, F. Najafi, X. Hu, and K. K. Berggren, "Numerical method to optimize the polar-azimuthal orientation of infrared superconducting-nanowire single-photon detectors", *Appl. Opt.*, **50**(29), 5949-5956 (2011)
8. X. Hu, C. W. Holzwarth, D. Masciarelli, E. A. Dauler, and K. K. Berggren, "Efficiently coupling light to superconducting nanowire single-photon detectors", *IEEE Trans. Appl. Supercond.*, **19**(3), 336-340 (2009)
9. X. Hu, E. A. Dauler, R. J. Molnar, and K. K. Berggren, "Superconducting nanowire single-photon detectors integrated with optical nano-antennae," *Opt. Express*, **19**(1), 17-31 (2011)
10. M. Csete, Á. Sipos, A. Szalai, G. Szabó: "Impact of polar-azimuthal illumination angles on efficiency of nano-cavity-array integrated single-photon detectors", *Optics Express*, **20**/15, 17065-17081 (2012)
11. M. Csete, Á. Sipos, A. Szalai, F. Najafi, G. Szabó, K. K. Berggren: "Improvement of infrared single-photon detectors absorptance by integrated plasmonic structures, submitted to *Scientific Reports*.
12. Y. Kurokawa, H. T. Miyazaki, "Metal-insulator-metal plasmon nanocavities: Analysis of optical properties", *Phys. Rev. B*, **75**, 035411 (2007)
13. A. Alú, G. D. Aguanno, N. Mattiucci, M. J. Bloemer: "Plasmonics Brewster Angle: Broadband Extraordinary Transmission through Optical Gratings", *Phys. Rev. Lett.* **106** 123902 (2011)
14. F. J. Garcia-Vidal and L. Martín-Moreno, "Transmission and focusing of light in one-dimensional periodically nanostructured metals," *Phys. Rev. B*, **66,** 155412 (2002)
15. D. Pacifici, H. J. Lezec, L A Sweatlock, R. J. Walters and H. A. Atwater, "Universal optical transmission features in periodic and quasiperiodic hole arrays", *Optics Express*, **16,** 9222-38 (2008)

7. Acknowledgements

The authors would like to thank the helpful discussions with Karl. K. Berggren, Faraz Najafi and Xiaolong Hu about the OC-SNSPDs and NCAI-SNSPDs.

The study was funded by the National Development Agency of Hungary with financial support form the Research and Technology Innovation Funds (OTKA CNK-78549), and OTKA K 75149. Mária Csete thanks the Balassi Institute for the Hungarian Eötvös post-doctoral fellowship.